www.elsevier.com/locate/talanta

Evaluation of two sterically directed attachments of biomolecules on a coaxial nanofibre membrane to improve the development of optical biosensors

Teresa Ramon-Marquez, Antonio L. Medina-Castillo, Alberto Fernandez-Gutierrez, Jorge F. Fernandez-Sanchez

PII: S0039-9140(18)30466-1
DOI: https://doi.org/10.1016/j.talanta.2018.05.004
Reference: TAL18644

To appear in: *Talanta*

Received date: 2 March 2018
Revised date: 25 April 2018
Accepted date: 1 May 2018

Cite this article as: Teresa Ramon-Marquez, Antonio L. Medina-Castillo, Alberto Fernandez-Gutierrez and Jorge F. Fernandez-Sanchez, Evaluation of two sterically directed attachments of biomolecules on a coaxial nanofibre membrane to improve the development of optical biosensors, *Talanta,* https://doi.org/10.1016/j.talanta.2018.05.004

Evaluation of two sterically directed attachments of biomolecules on a coaxial nanofibre membrane to improve the development of optical biosensors

Teresa Ramon-Marquez[1], Antonio L. Medina-Castillo[2], Alberto Fernandez-Gutierrez[1], Jorge F. Fernandez-Sanchez[1,*]

[1]Department of Analytical Chemistry, University of Granada, Avd. Fuentenueva s/n, 18071 Granada, Spain.

[2]NanoMyP®, Nanomateriales y Polimeros S.L., Spin-Off company of the UGR, BIC Building, Avd. Innovacion 1, E-18016, Granada, Spain.

*Corresponding author: jffernan@ugr.es

ABSTRACT

In this study, we have optimised the sterically directed attachment of biomolecules on the surface of coaxial membranes prepared by co-electrospinning which have been proved to be a material with very high performance for the development of biosensors with optical oxygen transduction. Uricase has been used as model enzyme.

Two sterically directed strategies: a) covalent attachment via maleimide, and b) affinity bonding via biotin-streptavidin interaction, have been tested in order to preserve the enzymatic activity of uricase and to improve the analytical figures of merits on the determination of uric acid. The best results were obtained with biotin-streptavidin affinity interaction and using a biotinylation reagent containing a polyethylene glycol chain. The developed biosensor showed high sensitivity towards uric acid with a detection limit of 0.5 μM, a quantification limit of 1.8 μM and linear range from 1.8 to 250 μM. The applicability of the membrane as biosensor with optical oxygen transduction was proved by determining uric acid in serum samples. The obtained results showed a good correlation (0.999) with those obtained by an external reference laboratory.

Graphical abstract

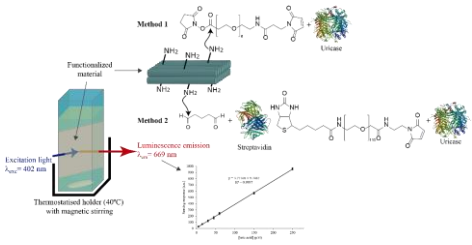

Graphical Abstracts

Keywords: Optical biosensor; Oxygen transduction; Multifunctional material; Biotin; Streptavidin; Uric acid.

1. Introduction

To develop biosensor membranes using optical oxygen transduction, a multifunctional material is required because it is necessary: 1) to immobilize a biomolecule which catalyses the oxidation of the analyte and 2) to incorporate an oxygen sensitive dye to measure the consumption of oxygen during this oxidation. In a previous work[1], we developed a multifunctional material based on co-electrospinning as a basic material for the development of biosensors with optical oxygen transduction (using uricase as model enzyme). It is based on coaxial nanofibres: an inner fibre containing an oxygen sensitive dye and an outer fibre containing aldehyde groups to allow the formation of Schiff bases with the amino groups of the uricase. However, the covalent attachment of uricase to the coaxial nanofibre membrane by aldehyde groups caused a high decrease in the relative activity of the enzyme and therefore, the sensitivity and the response time can be improved.

It is well-known that the method used for the immobilization of a biomolecule is a key factor that must be carefully optimised during the development of a biosensor [2-6]. Immobilization methods range broadly from physical methods, which include adsorption [7], encapsulation [8] and entrapment within a membrane [9], to more advanced chemical attachment procedures using chemically activated supports, which include covalent binding [2], crosslinking [10], and affinity interactions [11] between a functional group of the support (e.g. avidin, lectin, metal chelates) and a specific group (e.g. biotin, carbohydrate, histidine) of the biomolecule.

Covalent binding of biomolecules is a widely used immobilization method due to it allows achieving strong and efficient bonding between the biomolecules and the solid supports. This immobilization strategy is generally carried out by initial activation of the solid support followed by biomolecule coupling. In order to obtain good biological performances the linking of the biomolecule to the support has to be made through functional groups not essential for its biological activity. Thus, in this work, to improve the enzymatic performance of uricase, we have modified the previously described covalent attachment of uricase to the coaxial nanofibre membrane (based on the interaction of aldehyde groups of the support with amino groups of the biomolecule)[1], selecting reagents (maleimide) that can react with functional groups of the enzyme which are not implicated in its active site (thiol).

On the other hand, among the large variety of possible strategies for the immobilization of biomolecules on different supports, the specific biotin-(strept)avidin affinity interaction shows interesting advantages. The strong and specific non-covalent interaction between biotin and avidin or streptavidin leads to the formation of a high-affinity complex ($K_d \approx 10^{-15}$ M) with a strong association similar to the formation of a covalent bond. This interaction occurs very quickly and is highly resistant to wide ranges of pH, detergents, denaturing agents, organic solvents and high temperatures [12-14]. Furthermore, several studies have demonstrated that the immobilization based on the biotin-(strept)avidin affinity reaction results in the preservation of the biological activity of the immobilized molecules in a higher degree than other methods [15-17].

In addition, biotin can be easily covalently coupled to a large number of molecules by the carboxyl group of the valeric acid side chain. This group can be derivatized to incorporate several reactive groups that can be used to attach biotin to other biomolecules such as proteins, antibodies, polysaccharides, nucleic acids, etc. [18-20]. Thus, the small size of biotin makes it a perfect tag for biomolecules because biotinylation does not significantly alter their biological activity, and also the attaching to the valeric acid side chain does not usually interfere with the binding to streptavidin or avidin [20, 21]. Therefore, the immobilization of biomolecules on solid supports through the biotin-

(strept)avidin interaction is an exceptional tool for the different disciplines of biosciences, biomedicine and biotechnology [22-26].

In this study, we have carefully selected the reagents in order to preserve the enzymatic activity of the uricase by using these strategies. Moreover, the best strategy has been used to determine uric acid in serum samples and the results have been compared with the previous one obtained by immobilizing uricase via aldehyde interaction[1].

2. Experimental

2.1. Reagents and Materials

For the fabrication of the coaxial materials, PolymBlend® was kindly supplied by NanoMyp® (Granada, Spain, http://www.nanomyp.com); poly(methyl methacrylate) (PMMA) and *N*,*N*-dimethylformamide (DMF) were purchased from Sigma Aldrich, Madrid, Spain; Pd(II) meso-tetra(pentafluorophenyl)porphine (PdTFPP) was obtained from Frontier Scientific, Logan, UT, USA.

For the immobilization of uricase, potassium dihydrogen phosphate (KH_2PO_4), ethylenediamine (EDA), glutaraldehyde (GA), poly(ethylene glycol) [*N*-(2-maleimidoethyl)carbamoyl]methyl ether 2-(biotinylamino)ethane (biotin-PEG), maleimide-PEG_6-succinimidyl ester, *N*-biotinoyl-*N′*-(6-maleimidohexanoyl)hydrazide (biotin-maleimide), ethanolamine, uricase from *Candida* sp. (EC 1.7.3.3), and Tween 20 were all purchased from Sigma Aldrich, Madrid, Spain; streptavidin (SAv) from *Streptomyces avidinii* (expressed in *Escherichia coli*) was obtained from Nuptec (Zhejiang, China). All the solutions were prepared using doubly distilled water and used without further purification.

For the purification of biotinylated uricase, Zeba™ Spin Desalting Columns with a 7K molecular-weight cutoff were purchased from Thermo Fisher Scientific (Madrid, Spain, http://www.thermofisher.com), and Amicon® Ultra-4 centrifugal filters with a membrane NMWL of 10 kDa were obtained from Merck Millipore (Madrid, Spain, http://www.merckmillipore.com). To quantify the biotin label incorporation, 4´-hydroxyazobenzene-2-carboxylic acid (HABA) was purchased from Sigma Aldrich, Madrid, Spain.

To assay the activity of uricase, glycine, 4-aminoantipyrine (4-AAP), and peroxidase (HRP) from horseradish (EC 1.11.1.7) were purchased from Sigma Aldrich, Madrid, Spain, and uric acid and sodium 3,5-dichloro-2-hydroxybenzenesulfonate (DCHBS) were purchased from Alfa Aesar, Karlsruhe, Germany.

Human serum samples were obtained from a clinical analysis laboratory and stored frozen until assay.

2.2. Instrumentation

The UV-Visible absorption spectra were recorded on a Varian Cary 50 UV-Vis spectrophotometer. The luminescence measurements were carried out on a Varian Cary-Eclipse luminescence spectrophotometer.

All the luminescence measurements were carried out by controlling the temperature, which was continuously regulated by a commercial peltier cell holder connected to a temperature control module (Agilent Technologies, Madrid, Spain, www.agilent.com).

The morphological characterization of coaxial fibre membranes was done by TEM (Zeiss DSM 950) and SEM (LEO, Carl Zeiss, GEMINI-1530).

The pH of the buffer solutions was controlled using a digital pH meter (Crison micropH 2000) calibrated at 20 ± 2 ºC.

2.3.Fabrication of coaxial membranes

The fabrication of the coaxial nanofibre membranes was done by co-electrospinning following the procedure previously described by our research group [1]; Fig. 1 shows SEM and TEM pictures of the coaxial nanofibre mat. Briefly, two different polymeric solutions (10% w/w PolymBlend® in DMF and 6% w/w PMMA containing 1% w/w PdTFPP in DMF) were independently driven by two syringe pumps towards a single coaxial needle using a flow-rate of 1.3 and 0.3 mL h^{-1} for the outer (PolymBlend®) and inner (PMMA with PdTFPP) solutions, respectively, until reaching a concentric couple of stainless-steel capillary tubes (injector). Then, a potential difference between the injector and the collector (30 cm length and 20 cm diameter rotator drum located 25 cm apart from the injector and rotating at 400 rpm) was applied and the process was run for 8 h to collect membranes with thickness about 150 µm. After that, the obtained coaxial nanofibre membranes were submitted to a thermal wetting in distilled water in order to increase their hydrophilicity. Finally, the treated membranes were attached to adhesive sheets (Lohmann Technologies Corp.) to facilitate their handling; a scalpel was used to cut the material to a required size.

The resulting material has two functionalities: 1) a hydrophilic, functional, external area (outer fibre) which allows the chemical immobilisation of a biomolecule; and 2) a hydrophobic, internal zone (inner fibre) which contains a dissolved oxygen sensitive dye.

2.4. Immobilization of uricase on the coaxial nanofibre membrane

The immobilization of uricase on the coaxial nanofibre membrane was carried out by two different strategies, one by covalent immobilization and the other by biotin-streptavidin interaction:

1) For the covalent immobilization strategy: 20 cm^2 of material was first functionalized with vinyl active groups [27] and then with amino groups by using 0.9 M EDA in phosphate buffer (100 mM, pH 8.4) for 2.5 h at room temperature (RT) [28]. Then, amino groups were reacted with maleimide-PEG_6-succinimidyl ester by incubating 1.875 cm^2 of material with 4 mL of a solution of 0.75 mg mL^{-1} maleimide-PEG_6-succinimidyl ester in phosphate buffer (50 mM, pH 7.4) for different times (10, 20, 30, 60, 120 and 180 min) at RT in a rotating shaker. Then, it was washed with 5 mL of doubly distilled water (2x5 min).

   The covalent immobilization of uricase on this material was carried out by incubating 1.875 cm^2 of maleimide activated material with 4 mL uricase solution (20 µg mL^{-1}) in phosphate buffer (50 mM, pH 7.0) at 4 ºC for 20 h.

2) For the biotin-streptavidin interaction strategy: 20 cm^2 of material functionalized with vinyl active groups was reacted with 0.9 M EDA in phosphate buffer (100 mM, pH 8.4) for 45 min at RT. Then, amino groups were reacted with GA [28] by incubating 1.875 cm^2 of material with 5 mL of 15 % v/v GA solution in phosphate buffer (100 mM, pH 7.4) for 1 h at RT in a rotating shaker. After washing with doubly distilled water (3x10 min), the material was incubated with 2 mL of a solution of 125 μg mL^{-1} SAv in phosphate buffer (100 mM, pH 7.4) at 30 ºC for 24 h. Then, it was washed (3x10 min) with a solution containing 8.5 g L^{-1} of NaCl and 0.5 g L^{-1} of Tween 20 to remove all the no covalently bounded SAv.

   The free aldehyde groups of the material that had not reacted with SAv were blocked with a solution of 0.9 M ethanolamine in phosphate buffer (100 mM, pH 8) for 1 h at RT. Then the material was incubated with 4 mL of biotinylated uricase (5, 10, 15, 20, 40 and 80 μg mL^{-1}) in phosphate buffer (50 mM, pH 7.0) at 4 ºC for 20 h.

In both cases, after the incubation with uricase, the materials were washed with 4 mL phosphate buffer (15 min in a rotating shaker), and these washing solutions and the reaction supernatants were reserved for further testing. After washing with phosphate buffer, the materials were also washed (3x10 min) with the NaCl-Tween 20 solution. All these chemical modifications were carried out by submerging the materials (nonwoven mat attached to an adhesive sheet) in containers with the adequate volume to ensure that the entire material was submerged into the solution. The materials with immobilized uricase were stored in phosphate buffer (pH 7.4) at 4 ºC.

The amounts of SAv and uricase immobilized on the coaxial membrane were determined from the difference between the initial free amount and the total amount in the reaction supernatant and washing solutions after immobilization, assuming that the loss of biomolecule in each experiment is negligible. The biomolecule concentrations in the supernatant and washing solutions were measured by a spectrofluorometric method at 334 nm using a conventional luminescence cuvette [29].

2.5. Biotinylation of uricase

The incorporation of a biotin label to the uricase was carried out by using two different biotinylation reagents following the next procedure: 1.5 mL of a solution of 1.375 mg mL^{-1} uricase in phosphate buffer (50 mM, pH 7.0) was incubated with 0.5 mL of a solution of 12 mg mL^{-1} biotin-PEG or 2 mg mL^{-1} biotin-maleimide, in the same buffer at 4 ºC for 24 h. These chemical modifications were carried out by submerging the materials (nonwoven mat attached to an adhesive

sheet) in containers with the adequate volume to ensure that the entire material was submerged into the solution.

The level of biotin label incorporation was measured by a spectrophotometric method based on the strong biotin-SAv interaction [30]. The assay uses the ability of the dye HABA to bind to SAv originating a complex with an absorption peak at 500 nm. Since the affinity between HABA and SAv is relatively weak ($K_d \approx 10^{-4}$ M) compared to the affinity between biotin and SAv ($K_d \approx 10^{-15}$ M), biotin and biotinylated molecules can displace HABA from the HABA/SAv complex, resulting in a decrease in the absorption at 500 nm that can be related to the amount of biotin or biotinylated molecule in the sample.

Briefly, 500 µL of a solution containing SAv (0.2 mg mL^{-1}) and HABA (4 µg mL^{-1}) in phosphate buffer (100 mM, pH 7.4) were mixed with 12 µL of biotin solutions with different concentrations (0, 50, 100, 150, and 200 µg mL^{-1}) or 12 µL of unknown biotin concentration samples at RT for 5 min, and then the absorbance at 500 nm was measured using a conventional spectrophotometric cuvette.

2.6. Assay of the immobilized uricase activity

The relative activity (%) of the immobilized uricase was determined by a colorimetric method based on two enzymatic reactions [31]; relative activity is expressed as the percentage of the activity of the immobilised enzyme referred to the free enzyme (100% relative activity means that the activity of the bounded enzyme is the same than those of the free enzyme). The oxidation of uric acid catalysed by the action of uricase produces hydrogen peroxide, which reacts with DCHBS and 4-AAP in the presence of HRP to form a red quinoneimine dye with an absorption maximum at 513 nm. Based on this, the relative activity of uricase was calculated as a percentage of the immobilized uricase and free uricase absorbances.

In detail, to assay the activity of the immobilized uricase, 3 mL glycine buffer (50 mM, pH 8.8) containing 0.1 µmol uric acid were incubated with 1.875 cm^2 of coaxial with immobilized uricase for 20 min at 40 ºC. Then, 0.5 mL 4-AAP (10 mM), 0.5 mL DCHBS (50 mM) and 0.5 mL HRP (20 U mL^{-1}) in phosphate buffer (50 mM, pH 7.4) were added and kept at 40 ºC for 5 min to develop the colour. All the solutions were freshly prepared every day. The incubation procedure was carried out by submerging the material in a glass vial with the adequate volume to ensure that the entire material was submerged into the solution and the photometric measurement was done by measuring the absorbance of the supernatants using a conventional spectrophotometric cuvette.

2.7. Evaluation of the analytical features of the membrane and application

The determination of uric acid was indirectly determined by measuring the amount of oxygen consumed during the oxidation of uric acid by uricase [1]:

$$Uric\ acid + 2H_2O + O_2 \xrightarrow{Uricase} Allantoine + 2H_2O_2$$

The amount of oxygen consumed during this reaction can be determined by luminescence quenching which is described by the Stern–Volmer equation:

$$\frac{I_0}{I} = 1 + K_{SV} pO_2$$

where I_0 and I are the luminescence emission intensities from the membranes exposed to 100% N_2 and to different O_2 concentrations, respectively, K_{SV} is the Stern-Volmer constant and pO_2 is the oxygen partial pressure. Therefore, the increase of the luminescence signal of the oxygen sensitive dye incorporated into the inner fibre of the membrane can be related with the concentration of uric acid in the media.

Supporting Material (SM) shows the luminescence spectra of the material (see Fig. SM-1). The luminescence intensity of the dye increases with the concentration of uric acid due to the decrease in the dissolved oxygen concentration during the selective oxidation of uric acid by uricase. Fig. 2 shows the typical evolution of the luminescence response versus time when the membrane is exposed to uric acid.

The luminescence intensity was measured at excitation wavelength of 402 nm, emission wavelength of 669 nm, delay time (t_d) 200 µs, gate time (t_g) 5 ms, detector voltage 650 V and excitation and emission slits of 10 nm wide.

All the measurements were carried out by immersing the functionalised coaxial membranes into a conventional luminescence cuvette containing glycine buffer (50 mM, pH=8.8) and adding 40 µL of serum sample (final dilution 1:9, serum:buffer) or different volumes of 1 mM uric acid solution. The temperature was maintained at 40 ºC during the measurements. To allow the correct luminescence measurements the coaxial membranes must be placed having a disposition of 45º with both excitation and emission monochomators (SM shows a scheme of the measurement configuration; see Fig. SM-2).

The sensing response was calculated as the increase in the luminescence intensity when the membrane is exposed to uric acid or serum samples:

$$Sensing\ response = S_i - S_0$$

where S_i is the luminescence intensity at the plateau (4 min after uric acid is added) and S_0 is the luminescence signal before adding uric acid or serum sample (see Fig. 2).

In order to demonstrate the reliability of the developed sensing membrane, the obtained results for the four serum samples were compared with those determined by an accredited external laboratory (Análisis Clínicos Gilabert, Granada, Spain) by using the following colorimetric enzymatic method: uric acid is oxidised by uricase to allantoine and hydrogen peroxide ($2H_2O_2$), which under the influence of peroxidase (HRP), 4-aminophenazone (4-AP) and 2-4-dichlorophenol sulfonate (DCPS) forms a red quinoneimine compound (λ_{max}=520 nm):

$$Uric\ acid + 2H_2O + O_2 \xrightarrow{Uricase} Allantoine + 2H_2O_2$$

$$DCPS + 2H_2O_2 + 4\text{-}AP \xrightarrow{POD} Quinoneimine + 4H_2O$$

The intensity of the red colour formed is proportional to the uric acid concentration in the sample.

3. Results and discussion

3.1. Selection of the biotinylation reagents and the reagent for the covalent immobilization

In order to preserve the enzymatic activity of the uricase, the binding of the biotinylation reagent to the enzyme has to be carried out through amino acid residues of the enzyme that are not in its active site.

The active site of the uricase is delimited by arginine and glutamine residues that hold the substrate (uric acid) by H-bond, a phenylalanine residue that maintains a close π-stacking with the substrate, asparagine and threonine residues that build a peroxo hole for dioxygen, water, and hydrogen peroxide molecules [32, 33]. Therefore, the thiol side chain of cysteine residues is not implicated in the enzymatic activity of uricase and could be used to bind a biotin label. We selected biotin-PEG and biotin-maleimide as biotinylation reagents because their maleimido functional groups can react specifically with free sulfhydryls at pH 6.5-7.5 to form stable thioether bonds [34], which do not affect the enzymatic activity of the uricase.

On the other hand, the reagent used to attach the uricase by covalent immobilization was also selected to preserve the enzymatic activity of the enzyme. Thus, maleimide-PEG_6-succinimidyl ester which contains a maleimido functional group to react with free sulfhydryls of the uricase was selected.

3.2. Optimization of the immobilization of the enzyme on the coaxial nanofibre membrane

Two different strategies for the sterically directed immobilization of uricase on the coaxial membrane were evaluated to obtain the best sensing properties: 1) covalent attachment through a maleimide-PEG_6-succinimidyl ester linker; 2) biotin-streptavidin interaction by using biotin-maleimide or biotin-PEG as linkers.

For the covalent immobilization of the uricase to the membrane, a heterobifunctional crosslinker (maleimide-PEG_6-succinimidyl ester) with an ethylene oxide spacer (length = 31.7 Å) was used. The succinimidyl ester group of the crosslinker was first reacted with the amino groups of the material, whereas its maleimide functional group was subsequently used to form thioether directed bonds with free sulfhydryls of the uricase. The effect of the reaction time of crosslinker with the material (10, 20, 30, 60, 120 and 180 min) versus uricase immobilization was studied. The amount of immobilized enzyme and its relative activity versus reaction time are shown in SM (see Fig. SM-3). The relative activity of the enzyme decreases when the immobilized amount increases, obtaining the highest relative activity (36.5 %) at 10 min of reaction time. This relative activity is higher than that obtained in our previous work [1] by using the aldehyde interaction (18 %). This increase can be due to the selective reaction between the maleimide group of the crosslinker and the sulfhydryls of the uricase belonging to cysteine residues which are not implicated in the enzymatic activity, whereas the aldehyde groups react mainly with amino groups which could be part of the active site of the enzyme.

For the biotin-streptavidin immobilization of the uricase, the membrane has to be functionalized with streptavidin (SAv) and uricase must be labelled with biotin. The functionalization of the coaxial nanofibre membrane was done following the procedure described in Section 2.4 and two different biotinylation reagents (biotin-maleimide and biotin-PEG) with the same terminal functional groups but different spacer arm lengths (13 and 341 atoms from the biotin to the maleimide groups, respectively) were used to incorporate the biotin label to the uricase. The reactions to incorporate the biotin labels to the enzyme are described in Section 2.5. In both cases the amount of enzyme was the same but different amounts of biotinylation reagents were used because they have different solubility in phosphate buffer. The hydrophilic character of PEG spacer arm increases the solubility of the biotin-PEG reagent in the aqueous reaction media which allowed the use of a more concentrated solution of this reagent.

Two different devices (spin desalting columns and centrifugal filters) were tested for purification. The biotinylation level was quantified by the HABA method [30]. The highest biotinylation level was obtained with the biotin-PEG reagent. The biotinylation level was calculated by taking into

account the efficiency of the spin columns to purify the reaction solutions. Thus, solutions of both biotinylation reagents without enzyme were passed through the columns to determine their retention degree. The highest purification degree was obtained with the spin desalting column based on size exclusion for the biotin-maleimide reagent (80 % retention of reagent) and with the centrifugal filter for the biotin-PEG reagent (73 % retention of reagent).

The effect on the enzymatic activity of the purification step through the spin columns was also studied by measuring the activity of the enzyme in solution before and after the purification step. Fig. SM-4 shows that both, the use of the spin desalting column as well as the centrifugal filter, decreased the enzymatic activity (36 and 28 %, respectively). Therefore, in order to avoid this decrease in the activity of the enzyme, the incubation of the uricase, the biotinylation reagent and the streptavidin-functionalized membrane was performed in a single step.

The uricase biotinylated with the two biotinylation reagents were then incubated with the streptavidin-functionalized membrane following the procedure described in Section 2.4, and the amount of immobilized enzyme and its activity were evaluated (see SM, Fig. SM-5). The maximum amount of immobilized uricase was achieved with the biotin-maleimide reagent, but the highest relative activity of the enzyme was obtained with the biotin-PEG reagent for all the tested concentrations. These results indicate that the introduction of a longer spacer during the immobilization of uricase provides an improvement in the relative activity of the enzyme. Therefore, the distance from the surface of the membrane to the immobilized enzyme is a key factor to ensure a high enzymatic activity. This effect of the spacer on the enzyme activity can be due to the higher mobility of the enzyme in the presence of a longer spacer between the enzyme and the solid support [35, 36]; the increase in the mobility of the immobilized enzyme can favour the accessibility of the substrate to the enzyme, allowing a better interaction between them, and can reduce the influence of the solid surface on the enzyme and the alteration of the enzyme microenvironment. Thus, biotin-PEG with a poly(ethylene glycol) long linker was selected as the most adequate biotinylation reagent.

To determine the influence of the immobilized amount of streptavidin on the immobilization of biotinylated uricase, several SAv concentrations were tested (5, 25, 37.5, 50, 87.5, 125, 250 and 375 μg mL^{-1}) in phosphate buffer (100 mM, pH 7.4) at 30 ºC for 24 h. Fig. 3 shows that the amount of immobilized SAv increases linearly with the initial amount, maintaining an immobilization percentage between 76 and 89 % for all the tested concentrations.

Then the material was blocked for 1 h with a solution of 0.9 M ethanolamine, and subsequently it was incubated with 4 mL of biotin-PEG (60 μg mL^{-1}) and uricase (20 μg mL^{-1}) in phosphate buffer

(50 mM, pH 7.4) at 4 ºC for 20 h. The variation of the amount of immobilized uricase and its activity with the amount of immobilized SAv were also studied (see Fig. 4). This study shows that the amount of immobilized uricase is not practically affected by the amount of SAv on the membrane. This is probably because the amount of available SAv molecules is higher than the amount of biotinylated uricase. However, the relative activity of the uricase increases with the amount of SAv up to 36.0 % when the membrane contains 200 µg of immobilized SAv and then decreases. This variation could be due to the density of the affinity binding sites [36]. The increase in the amount of SAv molecules might lead to an increase in unspecific interactions that does not lead to an increase in the activity of the immobilized uricase, thus the control over the density of the affinity binding sites is essential to favour the specific binding. 200 µg of immobilised SAv (initial concentration of 125 µg mL^{-1} SAv) was selected as optimum to achieve the highest uricase relative activity. The obtained results indicated that the immobilized SAv retained its capacity to bind biotinylated conjugates and the incorporation of the biotin label to the uricase did not affect its activity or the ability of biotin to interact with SAv.

To optimise the concentration of uricase, the coaxial membrane functionalised with 125 µg mL^{-1} of SAv was incubated with 5 µg mL^{-1} biotin-PEG and different concentrations of uricase in phosphate buffer (50 mM, pH 7.0), resulting in different biotin-PEG:uricase molar ratios (1:0.25, 1:0.5, 1:1, 1:2, 1:3, 1:4, 1:5, 1:6, 1:7 and 1:8). Fig. 5 shows the variation of the amount of immobilised uricase and the absorbance of the red quinoneimine dye produced during the catalytic process (see section 2.6) which is related with the specific activity of the enzyme.

The amount of immobilized uricase increases with the initial amount of uricase, maintaining an immobilization percentage between 6.2 and 11.4 % for all the tested concentrations. However, the absorbance produced by catalytic action of immobilized uricase increases with the initial amount of uricase up to 260 µg and then it reaches a plateau. Therefore, an increase in the amount of immobilised uricase does not provide an increase of the compound produced by the catalytic action of immobilized uricase. It can be explained considering an unspecific adsorption of the uricase at concentrations higher than 65 µg mL^{-1} (initial amount of uricase of 260 µg); at low initial concentrations of uricase the immobilization is mostly produced by an affinity interaction due to the high amount of available streptavidin molecules; on the other hand, at high initial concentrations of uricase the steric hindrance produced by the immobilized uricase hinders the access to the rest of streptavidin molecules, causing an unspecific adsorption. Thus, the optimal initial concentration of uricase was set at 65 µg mL^{-1} (which corresponds with a biotin-PEG:uricase molar ratio of 1:2) in order to obtain low unspecific adsorption of the enzyme; at this molar ratio, the immobilization yield was 9.1 µg cm^{-2} and the relative enzymatic activity was 31.5 %.

The influence of the biotin-PEG concentration on the extent of uricase immobilization and the retention of its enzymatic activity was studied by maintaining the 1:2 biotin-PEG:uricase molar ratio and varying the concentration of biotin-PEG (from 1.3 to 25.6 μg mL^{-1}) during the incubation on the coaxial nanofiber membrane functionalised with 125 μg mL^{-1} SAv in phosphate buffer (50 mM, pH 7.0). The results of this experiment are shown in SM (see Fig. SM-6).

This experiment shows that when the biotin-PEG concentration is smaller than 8 μg mL^{-1} the amount of immobilized uricase is practically constant (from 9.5 to 14.1 μg) and the relative activity is high (from 35.2 to 41.4 %). At higher concentrations, the immobilization yield increases to reach a maximum at 43 μg cm^{-2} (80.8 μg of immobilized uricase), but the relative activity decreases considerably to 7.3 %. In this case (see Fig. SM-6b) the obtained absorbance signals also increase to reach a plateau suggesting that at biotin-PEG concentrations lower than 8 μg mL^{-1}, the unspecific adsorptions are relatively low, but at higher concentrations the immobilization of the enzyme is mostly unspecific, leading to a significant decrease in the relative activity. Thus, an initial biotin-PEG concentration of 8 μg mL^{-1} (corresponding with a SAv:biotin-PEG molar ratio 1:1.5) was selected. It provides a material with a relative enzymatic activity of 41.2 % and an immobilization yield of 8.1 μg cm^{-2}.

Therefore, the resulting membrane using the sterically directed strategy based on affinity bonding via biotin-streptavidin interaction (relative activity of 41.2 %) is a more active membrane than those obtained by covalent attachment via maleimide (36.5 % relative activity) or by non sterically directed strategy via aldehyde interaction (18 % relative activity; [1]). In addition, the selection of adequate molar ratios of biotin-PEG:uricase and SAv:biotin-PEG allows controlling the unspecific adsorption level, achieving a higher relative activity of the immobilized uricase.

3.3. Analytical figures of merits

In order to determine the response of the developed biosensor toward uric acid, the selected membranes were submerged in glycine buffer with different concentrations of uric acid and the evolution of the luminescence intensity with the time was registered (see Fig. 2). The luminescence intensity of the membranes increases when the concentration of uric acid in glycine buffer is also increased until to reach a plateau. The difference between the luminescence intensity after reaching the plateau and before adding the uric acid was used as sensing response to plot the calibration curve (see Fig. 6). The calibration curve was determined by measuring seven different concentrations of uric acid twice within three different membranes. The response time, determined as the time required for reaching the plateau from the addition of uric acid, was established as 5 min for all the membranes and all the tested concentrations. A linear relationship between the sensing response and

the uric acid concentration (linearity of 99.97%) was obtained in the range from 1.8 to 250 µM (see Fig. 6); slope of 3.77 μM^{-1} and intercept of 9.75. The detection and quantification limits were calculated using the IUPAC method (LOD=3s_b/m; LOQ=10s_b/m); where s_b is the standard deviation of 10 blanks and *m* is the slope of the calibration curve. The determined detection and quantification limits were 0.5 and 1.8 µM, respectively. Comparing these results with our previous publication using the same matrix but a different functionalization [1], it is possible to conclude that the biotin-SAv interaction improves considerably the sensitivity of the biosensing films; the slope of the calibration curve is increased from 0.11 to 3.77 μM^{-1} and the detection limit is reduced 8 times (from 4 to 0.5 µM). In comparison with other methods previously published for detecting uric acid (see Table 1) it is possible to conclude that the new biosensor based on biotin-SAv interaction and optical oxygen transduction is one of the most sensitive one; there are only two methods with a lower LOD (0.27 and 0.3 µM instead of 0.5 µM of the proposed biosensor) and none of them are optical.

3.4. Application

The developed membranes were employed for the determination of uric acid in four serum samples from healthy adults. Each serum sample was analysed with four different coaxial membranes following the procedure described in Section 2.7. The accuracy of the obtained results was tested by comparing the concentrations of uric acid in the serum samples calculated by the developed biosensor with those obtained by an external laboratory (reference method). Table 2 shows a comparison of the concentrations in serum samples determined by both methods. The values obtained by both methods showed a good correlation coefficient (0.999) with regression equation $y = 0.9107x + 17.03$ (Fig. SM-7). These results indicate that the developed membrane is an excellent biosensor for the accurate determination of uric acid in human serum, by using a small volume of serum (40 µL) and without any sample treatment.

4. Conclusions

In this study, we have demonstrated that biotin-SAv affinity interaction can be used to produce a sterically directed immobilization of uricase on the surface of coaxial fibers improving the analytical figures of merits of the coaxial nanofibre membrane with optical oxygen transduction developed by our research group.

The presence of molecules of SAv as binding points on the surface of the membrane enhanced the immobilization of uricase, and the use of biotin-PEG as biotinylation reagent allowed keep the immobilized enzyme at an adequate distance from the surface of the membrane. In addition, the

incubation of uricase and biotin-PEG with the streptavidin-functionalized membrane can be done in one single step, avoiding purification steps and reducing loss of enzymatic activity.

In order to achieve the best enzymatic activity, the immobilization of uricase on the coaxial membrane was optimized selecting adequate biotin-PEG:uricase (1:2) and SAv:biotin-PEG (1:1.5) molar ratios, which allowed obtain a relative enzymatic activity of 41.2 %, higher than those obtained via maleimide (36.5 %) and aldehyde (18 %) interactions.

The developed sensing membrane provides good analytical figures (detection limit of 0.5 μM, quantification limit of 1.8 μM, and linear range from 1.8 to 250 μM) and can be used to determine the uric acid concentration in serum samples without any sample treatment. The obtained results analysing serum samples with the developed membrane were compared with those obtained by an external reference laboratory, achieving a good correlation (0.999) which demonstrates its applicability as biosensor with optical oxygen transduction.

This material could also be used for the immobilization of other enzymes and for hosting other dyes, which could originate interesting applications in the field of biosensing and help to solve the problem of sensitivity of several optical sensing films.

Acknowledgments

This work has received funding from the People Programme (Marie Curie Actions, Multi-ITN) of the European Union's Seventh Framework Programme for research, technological development and demonstration under grant agreement n° 608104 (EUROMBR) and the Spanish Ministry of Economy and Competitiveness (Ramon-Marquez's grant reference AP2012-0944, Medina-Castillo's Torres Quevedo contract reference PTQ-11-04904 and project CTQ2014-53442-P).

References

[1] T. Ramon-Marquez, A.L. Medina-Castillo, N. Nagiah, A. Fernandez-Gutierrez, J.F. Fernandez-Sanchez, A multifunctional material based on co-electrospinning for developing biosensors with optical oxygen transduction, Analytica Chimica Acta 1015 (2018) 66-73.
[2] A. Sassolas, L.J. Blum, B.D. Leca-Bouvier, Immobilization strategies to develop enzymatic biosensors, Biotechnology Advances 30(3) (2012) 489-511.
[3] T. Ahuja, I.A. Mir, D. Kumar, Rajesh, Biomolecular immobilization on conducting polymers for biosensing applications, Biomaterials 28(5) (2007) 791-805.

[4] A. Tereshchenko, M. Bechelany, R. Viter, V. Khranovskyy, V. Smyntyna, N. Starodub, R. Yakimova, Optical biosensors based on ZnO nanostructures: advantages and perspectives. A review, Sensors and Actuators B: Chemical 229 (2016) 664-677.
[5] E.A.H. Hall, S. Chen, J. Chun, Y. Du, Z. Zhao, A molecular biology approach to protein coupling at a biosensor interface, TrAC Trends in Analytical Chemistry 79 (2016) 247-256.
[6] Y. Gao, I. Kyratzis, Covalent Immobilization of Proteins on Carbon Nanotubes Using the Cross-Linker 1-Ethyl-3-(3-dimethylaminopropyl)carbodiimide—a Critical Assessment, Bioconjugate Chemistry 19(10) (2008) 1945-1950.
[7] D. Samanta, A. Sarkar, Immobilization of bio-macromolecules on self-assembled monolayers: methods and sensor applications, Chemical Society Reviews 40(5) (2011) 2567-2592.
[8] K. Edwards, M. Kato, N. Utsunomiya-Tate, T. Toyo'oka, Encapsulated Biomolecules Using Sol-Gel Reaction for High-Throughput Screening, Frontiers in Drug Design & Discovery (2006) 273-294.
[9] M.R.N. Monton, E.M. Forsberg, J.D. Brennan, Tailoring Sol–Gel-Derived Silica Materials for Optical Biosensing, Chemistry of Materials 24(5) (2012) 796-811.
[10] S. Talekar, A. Joshi, G. Joshi, P. Kamat, R. Haripurkar, S. Kambale, Parameters in preparation and characterization of cross linked enzyme aggregates (CLEAs), RSC Advances 3(31) (2013) 12485-12511.
[11] B. Prieto-Simon, M. Campas, J.L. Marty, Biomolecule Immobilization in Biosensor Development: Tailored Strategies Based on Affinity Interactions, Protein and Peptide Letters 15(8) (2008) 757-763.
[12] M.D. Savage, An Introduction to Avidin-Biotin Technology and Options for Biotinylation, in: T. Meier, F. Fahrenholz (Eds.), A Laboratory Guide to Biotin-Labeling in Biomolecule Analysis, Birkhäuser Basel, Basel, 1996, pp. 1-29.
[13] E.P. Diamandis, T.K. Christopoulos, The biotin-(strept)avidin system: principles and applications in biotechnology, Clinical Chemistry 37(5) (1991) 625-636.
[14] H. Sakahara, T. Saga, Avidin–biotin system for delivery of diagnostic agents, Advanced Drug Delivery Reviews 37(1–3) (1999) 89-101.
[15] H. Schetters, Avidin and streptavidin in clinical diagnostics, Biomolecular Engineering 16(1–4) (1999) 73-78.
[16] B. Limoges, J.-M. Savéant, D. Yazidi, Quantitative Analysis of Catalysis and Inhibition at Horseradish Peroxidase Monolayers Immobilized on an Electrode Surface, Journal of the American Chemical Society 125(30) (2003) 9192-9203.
[17] M. Amounas, C. Innocent, S. Cosnier, P. Seta, A membrane based reactor with an enzyme immobilized by an avidin–biotin molecular recognition in a polymer matrix, Journal of Membrane Science 176(2) (2000) 169-176.
[18] G. Elia, Protein Biotinylation, Current Protocols in Protein Science, John Wiley & Sons, Inc.2001.
[19] B.K. Kay, S. Thai, V.V. Volgina, High-throughput Biotinylation of Proteins, Methods in molecular biology (Clifton, N.J.) 498 (2009) 185-196.
[20] G.T. Hermanson, Chapter 11 - (Strept)avidin–Biotin Systems, Bioconjugate Techniques (Third edition), Academic Press, Boston, 2013, pp. 465-505.
[21] G. Elia, Biotinylation reagents for the study of cell surface proteins, PROTEOMICS 8(19) (2008) 4012-4024.
[22] Z. Liu, L. Jiang, F. Galli, I. Nederlof, R.C.L. Olsthoorn, G.E.M. Lamers, T.H. Oosterkamp, J.P. Abrahams, A Graphene Oxide˙Streptavidin Complex for Biorecognition – Towards Affinity Purification, Advanced Functional Materials 20(17) (2010) 2857-2865.
[23] B. Lin, J. Qiu, J. Gerstenmeier, P. Li, H. Pien, J. Pepper, B. Cunningham, A label-free optical technique for detecting small molecule interactions, Biosensors and Bioelectronics 17(9) (2002) 827-834.

[24] J. Liu, Y. Ye, Z. Hu, Y. Zou, G. Chen, L. Yu, A hypersensitive biotin-avidin-TRFIA for quantitative detection of ANA-Ig(GAM) and its clinical application, Journal of Immunoassay and Immunochemistry 34(2) (2013) 197-207.
[25] R.N. Orth, T.G. Clark, H.G. Craighead, Avidin-Biotin Micropatterning Methods for Biosensor Applications, Biomedical Microdevices 5(1) (2003) 29-34.
[26] Z. Yang, J. Shen, J. Li, J. Zhu, X. Hu, An ultrasensitive streptavidin-functionalized carbon nanotubes platform for chemiluminescent immunoassay, Analytica Chimica Acta 774 (2013) 85-91.
[27] A.L. Medina-Castillo, J. Morales-Sanfrutos, A. Megia-Fernandez, J.F. Fernandez-Sanchez, F. Santoyo-Gonzalez, A. Fernandez-Gutierrez, Novel synthetic route for covalent coupling of biomolecules on super-paramagnetic hybrid nanoparticles, Journal of Polymer Science Part A: Polymer Chemistry 50(19) (2012) 3944-3953.
[28] J.M. Goddard, J.H. Hotchkiss, Polymer surface modification for the attachment of bioactive compounds, Progress in Polymer Science 32(7) (2007) 698-725.
[29] M.S. Caves, B.K. Derham, J. Jezek, R.B. Freedman, Thermal Inactivation of Uricase (Urate Oxidase): Mechanism and Effects of Additives, Biochemistry 52(3) (2013) 497-507.
[30] N.M. Green, [74] Spectrophotometric determination of avidin and biotin, Methods in Enzymology, Academic Press1970, pp. 418-424.
[31] T. Ramon-Marquez, A.L. Medina-Castillo, J.F. Fernandez-Sanchez, A. Fernandez-Gutierrez, Evaluation of different functional groups for covalent immobilization of enzymes in the development of biosensors with oxygen optical transduction, Analytical Methods 7(7) (2015) 2943-2949.
[32] L. Gabison, C. Chopard, N. Colloc'h, F. Peyrot, B. Castro, M.E. Hajji, M. Altarsha, G. Monard, M. Chiadmi, T. Prangé, X-ray, ESR, and quantum mechanics studies unravel a spin well in the cofactor-less urate oxidase, Proteins: Structure, Function, and Bioinformatics 79(6) (2011) 1964-1976.
[33] L. Gabison, T. Prangé, N. Colloc'h, M. El Hajji, B. Castro, M. Chiadmi, Structural analysis of urate oxidase in complex with its natural substrate inhibited by cyanide: Mechanistic implications, BMC Structural Biology 8(1) (2008) 32.
[34] G.T. Hermanson, Chapter 6 - Heterobifunctional Crosslinkers, Bioconjugate Techniques (Third edition), Academic Press, Boston, 2013, pp. 299-339.
[35] J.N. Talbert, J.M. Goddard, Enzymes on material surfaces, Colloids and Surfaces B: Biointerfaces 93 (2012) 8-19.
[36] L. Cao, Covalent Enzyme Immobilization, Carrier-bound Immobilized Enzymes, Wiley-VCH Verlag GmbH & Co. KGaA2006, pp. 169-316.
[37] Y. Zhang, G. Wen, Y. Zhou, S. Shuang, C. Dong, M.M.F. Choi, Development and analytical application of an uric acid biosensor using an uricase-immobilized eggshell membrane, Biosensors and Bioelectronics 22(8) (2007) 1791-1797.
[38] K. Arora, G. Sumana, V. Saxena, R.K. Gupta, S.K. Gupta, J.V. Yakhmi, M.K. Pandey, S. Chand, B.D. Malhotra, Improved performance of polyaniline-uricase biosensor, Analytica Chimica Acta 594(1) (2007) 17-23.
[39] R. Rawal, S. Chawla, N. Chauhan, T. Dahiya, C.S. Pundir, Construction of amperometric uric acid biosensor based on uricase immobilized on PBNPs/cMWCNT/PANI/Au composite, International Journal of Biological Macromolecules 50(1) (2012) 112-118.
[40] K. Jindal, M. Tomar, V. Gupta, CuO thin film based uric acid biosensor with enhanced response characteristics, Biosensors and Bioelectronics 38(1) (2012) 11-18.
[41] R. Mundaca-Uribe, F. Bustos-Ramírez, C. Zaror-Zaror, M. Aranda-Bustos, J. Neira-Hinojosa, C. Peña-Farfal, Development of a bienzymatic amperometric biosensor to determine uric acid in human serum, based on mesoporous silica (MCM-41) for enzyme immobilization, Sensors and Actuators B: Chemical 195(Supplement C) (2014) 58-62.

[42] Y. Zhang, M. Yan, P. Gao, J. Jiang, G. Zhang, J. Li, S. Shuang, Immobilization of uricase-gold nanoparticles composite nanomaterial on a biofilm and its application to determination of uric acid, Applied Biochemistry and Microbiology 51(4) (2015) 470-478.
[43] F.S. da Cruz, F.d.S. Paula, D.L. Franco, W.T.P. dos Santos, L.F. Ferreira, Electrochemical detection of uric acid using graphite screen-printed electrodes modified with Prussian blue/poly(4-aminosalicylic acid)/Uricase, Journal of Electroanalytical Chemistry 806 (2017) 172-179.
[44] Y. Zhao, X. Wei, N. Peng, J. Wang, Z. Jiang, Study of ZnS Nanostructures Based Electrochemical and Photoelectrochemical Biosensors for Uric Acid Detection, Sensors 17(6) (2017) 1235.
[45] B. Peng, J. Cui, Y. Wang, J. Liu, H. Zheng, L. Jin, X. Zhang, Y. Zhang, Y. Wu, CeO2-x/C/rGO nanocomposites derived from Ce-MOF and graphene oxide as a robust platform for highly sensitive uric acid detection, Nanoscale 10(4) (2018) 1939-1945.
[46] H.-c. Tsai, R.-a. Doong, Simultaneous determination of renal clinical analytes in serum using hydrolase- and oxidase-encapsulated optical array biosensors, Analytical Biochemistry 334(1) (2004) 183-192.
[47] P. Schrenkhammer, O.S. Wolfbeis, Fully reversible optical biosensors for uric acid using oxygen transduction, Biosensors and Bioelectronics 24(4) (2008) 994-999.
[48] K. Phaugat, M. Bhambi, Renu, C.S. Pundir, Polyethylene terephthalate membrane as a support for covalent immobilization of uricase and its application in serum urate determination, Journal of Molecular Catalysis B: Enzymatic 62(1) (2010) 27-31.
[49] G. Bayramoğlu, A.Ü. Metin, M.Y. Arıca, Surface modification of polyacrylonitrile film by anchoring conductive polyaniline and determination of uricase adsorption capacity and activity, Applied Surface Science 256(22) (2010) 6710-6716.
[50] D. Yao, A.G. Vlessidis, N.P. Evmiridis, Microdialysis sampling and monitoring of uric acid in vivo by a chemiluminescence reaction and an enzyme on immobilized chitosan support membrane, Analytica Chimica Acta 478(1) (2003) 23-30.
[51] C.M. Miyazaki, F.M. Shimizu, J.R. Mejía-Salazar, O.N. Oliveira, M. Ferreira, Surface plasmon resonance biosensor for enzymatic detection of small analytes, Nanotechnology 28(14) (2017).

Fig. 1. Images of a) SEM and b) TEM of the multifunctional coaxial membrane formed by PMMA-PdTFPP as inner fibre and PolymBlend® as outer fibre.

Fig. 2. Luminescence response of the biosensor membrane when it is exposed to uric acid and example of determination of the sensing response; solid line corresponds to the luminescence emission of the functionalised material and dashed line is the luminescence of the unmodified coaxial material.

Fig. 3. Effect of the initial amount of SAv on the amount (grey line) and immobilization percentage (black line) of immobilised SAv. Errors are calculated as $^{st}/_{\sqrt{n}}$ where *s* is the standard deviation, *t* is the student t for 95% probability and *n-1* freedom degrees, and *n* is the number or replicas (at least 3 replicas in each case).

Fig. 4. Effect of the amount of immobilised SAv on the relative enzymatic activity (grey line) and amount (black line) of immobilised uricase. Errors are calculated as $^{st}/_{\sqrt{n}}$ where *s* is the standard deviation, *t* is the student t for 95% probability and *n-1* freedom degrees, and *n* is the number or replicas (at least 3 replicas in each case).

Fig. 5. Effect of the initial amount of uricase on the amount of immobilised uricase (black line) and the absorbance of the red quinoneimine dye at 513 nm (grey line). Errors are calculated as $^{st}/_{\sqrt{n}}$ where *s* is the standard deviation, *t* is the student t for 95% probability and *n-1* freedom degrees, and *n* is the number or replicas (at least 3 replicas in each case).

Fig. 6. Analytical calibration curve. Errors are calculated as $^{st}/_{\sqrt{n}}$ where *s* is the standard deviation, *t* is the student t for 95% probability and *n-1* freedom degrees, and *n* is the number or replicas (at least 3 replicas in each case).

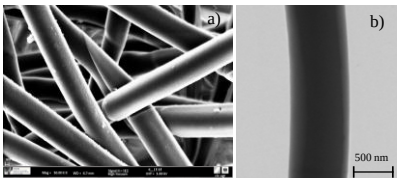

Figure 1

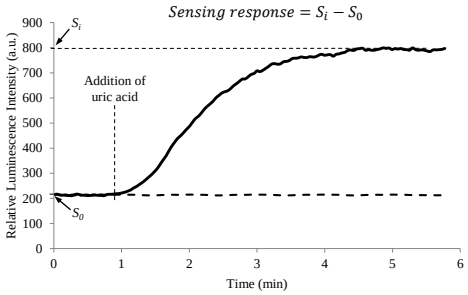

Figure 2

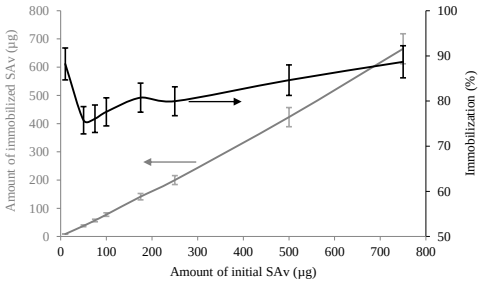

Figure 3

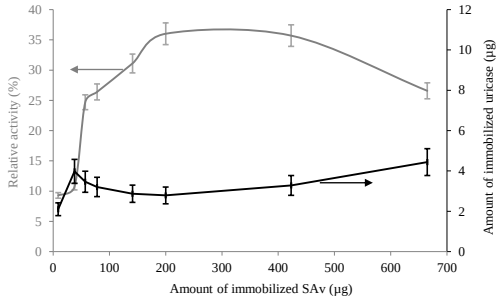

Figure 4

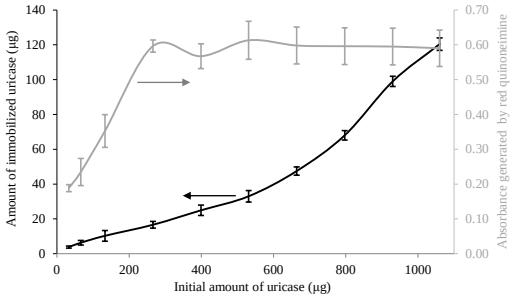

Figure 5

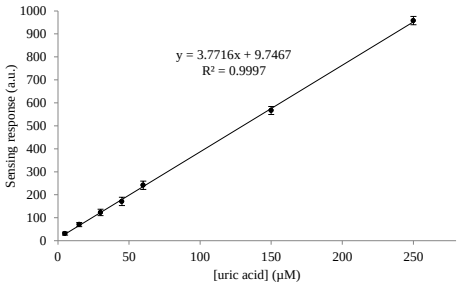

Figure 6

Table 1. Comparison of the proposed biosensor with other previously published in the literature.

Detection method	LOD (µM)	Linear range (µM)	Immobilization Method	Matrix	Ref.
Amperometry	2	4.0-	Covalent	Eggshell	[37]
Amperometry	10	10-600	Covalent	Polyaniline	[38]
Amperometry	5	5-800	Crosslinking/adsorption	Chitosan, carbon	[39]
Amperometry	140	50-	Adsorption	Copper oxide	[40]
Amperometry	0.33	2-10	Entrapment	Mesoporous	[41]
Amperometry	0.8	1.0–	Covalent	Gold	[42]
Amperometry	3.0	10–	Adsorption	Carbon graphite	[43]
Amperometry	1.79	10–	Entrapment	ZnS	[44]
Amperometry	2.0	49.8–	Adsorption	Cerium and	[45]
Fluorometry	25	10-	Sol-gel entrapment	Polyvinylalcohol	[46]
Fluorometry	5	5-800	Entrapment	Polyurethane	[47]
Spectrophotometry	50	50-500	Covalent	Polyethylene	[48]
Spectrophotometry	5.67	5.67-	Adsorption	Polyacrylonitrile	[49]
Chemiluminescence	5	10-	Affinity	Chitosan	[50]
Surface plasmon resonance	0.27	–	Layer-by-layer	Poly(ethylene imine) and microperoxidase-11	[51]
Luminescence	4	15-500	Covalent	PolymBlend®	[1]
Luminescence	0.5	1.8-	Biotin-SAv interaction	PolymBlend®	This work

Table 2. Results of the uric acid determination by the proposed biosensor and an external reference laboratory.

Sample	[uric acid] (µM) External reference laboratory	[uric acid] (µM) Proposed biosensor[a]
1	220.1	218.5 ± 12.6
2	190.4	191.6 ± 3.9
3	148.7	152.0 ± 5.5
4	220.1	215.7 ± 6.9

[a] Four different coaxial membranes per sample were used to determine the uric acid concentration

Highlights

- Optimization the sterically directed attachment of biomolecules on multifunctional material
- Uricase has been selected as model enzyme.
- It shows a detection limit of 0.5 µM and a linear range of 0.5-250 µM
- The most sensitive optical method for analysing uric acid
- It has been used for detecting uric acid in serum samples